Rare Metal Materials and Engineering
Volume 51, Issue 9, September 2022
Available online at www.rmme.ac.cn

Science Press

Cite this article as: Ma Guofeng, Li Hui, Liu Zhiyang, et al. High-Temperature Oxidation Properties of Micro-arc Oxidation Film on 2A12 Aluminum Alloy[J]. Rare Metal Materials and Engineering, 2022, 51(09): 3166-3171.

ARTICLE

High-Temperature Oxidation Properties of Micro-arc Oxidation Film on 2A12 Aluminum Alloy

Ma Guofeng, Li Hui, Liu Zhiyang, Sun Shineng, Wang Ziyao

Shenyang University, Shenyang 110044, China

Abstract: The high-temperature oxidation experiments were conducted on the micro-arc oxidation film on 2A12 aluminum alloy surface. Results show that the high-temperature oxidation resistance of the micro-arc oxidation film is decreased with increasing the temperature. However, the oxidation index is above 2, indicating that the micro-arc oxidation film has a protective effect for the 2A12 aluminum alloy and can effectively prevent the oxygen diffusion during high-temperature oxidation. The air-cooled thermal shock resistance property of the micro-arc oxidation film layer is better than its water-cooled thermal shock resistance property. After 60 thermal shock cycles, the film falls off at the corners of alloy after water-cooled thermal shock, while only cracks appear on the surface of alloy after air-cooled thermal shock without film shedding. The failure of micro-arc oxidation film after thermal shock is mainly caused by the difference in coefficients of thermal expansion between film and substrate and the formation of hydroxides and oxides through the reactions of film with H_2O and oxygen, respectively. The CeO_2 inside the film can reduce the pore size and the impact of thermal shock on the film at the initial reaction stage. However, with increasing the thermal shock cycles, the subcarbonate and hydroxide are generated, leading to the failure of micro-arc oxidation film.

Key words: high-temperature oxidation resistance property; micro-arc oxidation film; thermal shock resistance; rare earth oxide additive

Aluminum alloys have been widely used in the aerospace industry, automobile industry, and electronic products, owing to their high specific strength, great machinability, and excellent heat and electric conductivity. However, the low hardness and toughness, inferior abrasion and shock resistance, relatively high heat conductivity coefficient and thermal deformation, and poor thermal stability all restrict the application of aluminum alloys. In order to apply aluminum alloys on engine manufacture, the preparation of film with high-temperature resistance and thermal shock resistance on the aluminum alloy surface is of great importance.

Micro-arc oxidation (MAO) technique can form a layer of ceramic membrane, which mainly consists of the matrix metal oxides on the metal surface. By regulating the electrolyte and corresponding electrical parameters, the instantaneous high temperature and pressure are generated by the arc strike on the metal matrix and the alloy surface[1,2]. The generated ceramic membranes usually have better comprehensive mechanical and chemical properties, such as high hardness and excellent corrosion and abrasion resistance. Thus, the high-temperature oxidation resistance and thermal shock resistance of MAO layer were investigated in this research.

Rare earth elements are commonly used in the surface treatment to enhance the properties of oxidants or catalysts. Traditionally, the alloy is simply immersed in the rare earth saline solution for MAO film preparation, which leads to few rare earth elements on the matrix surface, i. e., the advantages of rare earth element addition cannot be revealed. Therefore, the surface density and corrosion resistance of this kind of MAO film should be further improved[3].

In this research, the rare earth oxide CeO_2 was added into the electrolyte for MAO film preparation on the surface of 2A12 aluminum alloy. The mechanisms of high-temperature oxidation and thermal shock resistance of MAO film were investigated to provide guidance for the protection of 2A12 aluminum alloy.

1 Experiment

The chemical composition of 2A12 aluminum alloy is shown in Table 1[4]. The specimens were uniformly cut into

Received date: September 06, 2021
Foundation item: Liaoning Provincial Natural Science Foundation (2019-MS-236); Shenyang Science and Technology Project (20-202-1-12)
Corresponding author: Ma Guofeng, Ph. D., Professor, Shenyang University, Shenyang 110044, P. R. China, Tel: 0086-24-62269852, E-mail: guofma@163.com

rectangle plates with the size of 25 mm×20 mm×1.5 mm by spark wire cutting. Punch a hole on the specimen to connect the wire. Firstly, the specimen was mechanically polished and then polished with water-based sandpaper from 400# to 1500#. After the polishing process, the ultrasonic cleaner was used to clean the specimen in absolute ethanol for 20 min. Then, a hair dryer was used to dry the specimen. The stainless steel was used as the negative electrode of the experiment. The power supply was the pulse power, and the related parameters are shown in Table 2. The electrolyte was prepared with deionized water, and its composition is shown in Table 3. The low-temperature thermostat was used to control the reaction temperature at 25±5 °C.

The high-temperature oxidation experiments were conducted in a muffle furnace. Firstly, the ceramic crucible was put into the resistance furnace for preheating, and then the specimens were weighed and put into the crucible. The heating duration was 2, 4, 6, 8, and 10 h. The temperature was kept at 400, 450, and 500 °C. After the specimens were air-cooled to room temperature, the specimen mass was measured to calculate the mass gain. The surface morphology was observed by scanning electron microscope (SEM)[5].

The thermal shock experiments were conducted under the conditions of air-cooling and water-cooling separately. The reaction occurred in the resistance furnace, and the thermal shock stability was evaluated by the number of thermal shock cycles when the alloy surface was damaged. Under the air-cooling condition, the specimen was put into a preheated ceramic crucible, kept for 5 min, and then taken out. After air-cooling for 3 min, the specimen was placed into the ceramic crucible again. The experiment temperature was 550 °C. Under the water-cooling condition, the specimen was put into a preheated ceramic crucible, kept at 550 °C for 5 min, and then immersed in water for quenching.

2 Results and Discussion

2.1 Surface microstructure after high-temperature oxidation

Fig. 1 shows SEM surface morphologies of the MAO films after oxidation at 400 °C for different durations. After oxidation at 400 °C for 2 h, no obvious changes can be observed on the MAO film surface, which is mainly attributed to the less severe oxidation condition and uniformly distributed crater-formed pores, whose size is relatively consistent[6]. With prolonging the oxidation duration to 4 h, a large number of microcracks appear and the surface is obviously rougher than the original surface. However, due to the relatively low oxidation temperature, no obvious propagation of the microcracks occurs. With prolonging the oxidation duration to 6 and 8 h, the cracks on the surface are further increased and the crack width is also increased. With prolonging the oxidation duration to 10 h, the surface of MAO film begins to fracture.

Fig. 2 shows SEM surface morphologies of the MAO films after oxidation at 450 °C for different durations. After oxidation at 450 °C for 2 h, the cracks appear on the surface and pass through the pores[7-9]. The longer the oxidation duration, the larger the crack width. The fracture occurs after oxidation for 10 h[10].

Fig. 3 shows SEM surface morphologies of the MAO films after oxidation at 500 °C for different durations. Because the temperature is higher, the surface morphology of MAO film changes more easily than that oxidized at relatively lower temperature does. It can be seen that the surface changes from white (original surface) to sepia accompanied by the appearance of black spots[11-13]. With prolonging the oxidization duration, the roughness and the number of black spots on MAO film surface are increased, and the width and length of the microcracks are also increased. This phenomenon results from the sustaining stress during the high-temperature oxidation. Besides, during the air- and water-cooling processes, the air and water enter the film through the pores on the surface and react with the film layer and aluminum alloy matrix to form granular oxide, which grows into lamellar oxide with prolonging the oxidation duration. The stacking occurs when the number of lamellar oxides is increased, resulting in the rougher surface of MAO film. Therefore, reducing the pore size is a key factor to improve the oxidation resistance of MAO film at high temperatures[14,15].

By adding CeO_2 particles into the electrolyte, the pore size of the MAO film surface is effectively reduced, thus decreasing the amount of air or water which is in contact with the matrix. With the oxidation proceeding, the rare earth oxide gradually becomes subcarbonate, thereby losing the efficacy[16]. The related reaction is as follows:

$$CeO_2+CO_2+H_2O\rightarrow Ce(CO_3)_2\cdot Ce(OH)_3 \quad (1)$$

The rare earth oxide can also react with H_2O to produce hydroxide, as follows:

$$CeO_2+H_2O\rightarrow CeO(OH) \quad (2)$$

$$CeO_2+H_2O\rightarrow Ce(OH)_3 \quad (3)$$

The generated subcarbonate and hydroxide accumulate with prolonging the oxidation duration. When the generated

Table 1 Chemical composition of 2A12 aluminum alloy[4] (wt%)

Si	Cu	Mg	Zn	Mn	Ti	Ni	Fe	Al
≤0.50	3.80~4.90	1.20~1.80	≤0.30	0.30~0.90	≤0.15	≤0.10	≤0.50	Bal.

Table 2 Power supply parameters

Positive voltage/V	Negative voltage/V	Positive pulse width/ms	Negative pulse width/ms	Pulse interval/ms	Time/s
300	80	1000	1000	300	900

Table 3 Composition of electrolyte ($g \cdot L^{-1}$)

Na_2SiO_3	KOH	CeO_2
15	5	3

products reach a certain amount, the internal thermal stress will form and expand the microcracks. When the oxidation duration reaches 10 h, the surface film layer is separated by microcracks, which is connected to the crater-formed pores. Therefore, the H_2O and CO_2 easily enter the inner layer, the accumulation of lamellar oxides is accelerated, and more rare earth oxides are generated at high temperatures. Due to the internal stress, the MAO film layer falls off.

2.2 Mass gain after high-temperature oxidation and kinetic analysis

Fig.4 illustrates the mass change curves of MAO films after oxidation at different temperatures. It can be seen that after oxidation at 400 °C for 2 h, the mass does not change, which is consistent with the morphology observation results. With prolonging the oxidation duration to 4 h, the mass is increased by 0.000 04 g/cm^2. The mass gain is 0.000 06 g/cm^2 when the oxidation duration is 6 h. When the oxidation duration is 8 h, the mass gain is 0.000 04 g/cm^2. When the oxidation duration is 10 h, the mass declines obviously due to the shedding of the surface film.

After oxidation at 450 °C for 2 h, the mass gain is 0.000 02

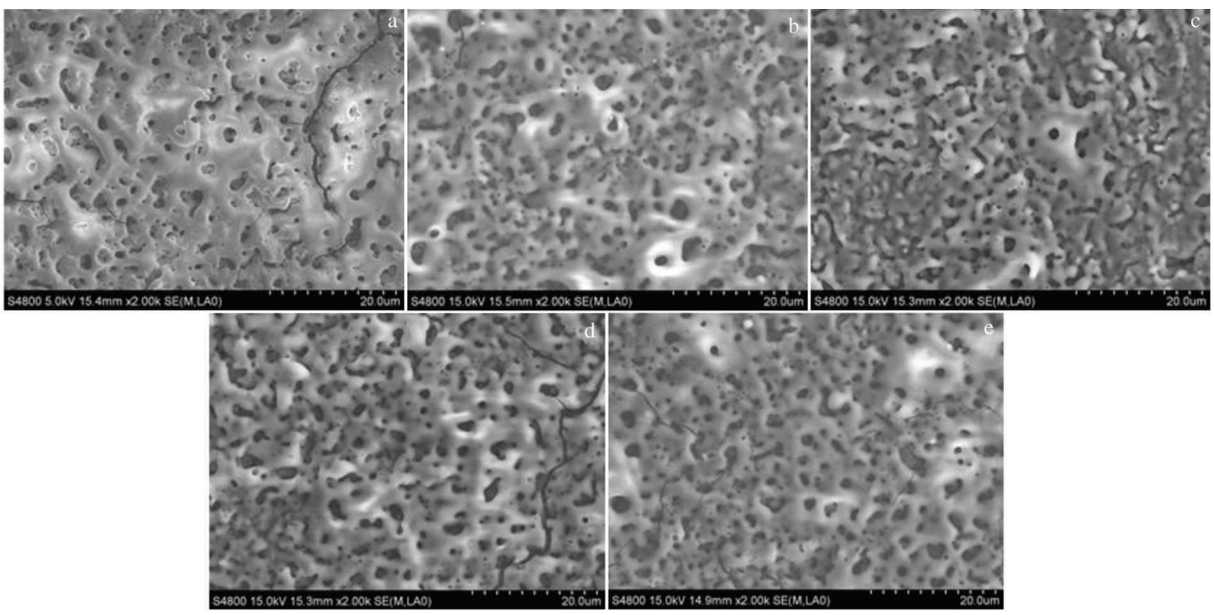

Fig.1 SEM surface morphologies of MAO films after oxidation at 400 °C for 2 h (a), 4 h (b), 6 h (c), 8 h (d), and 10 h (e)

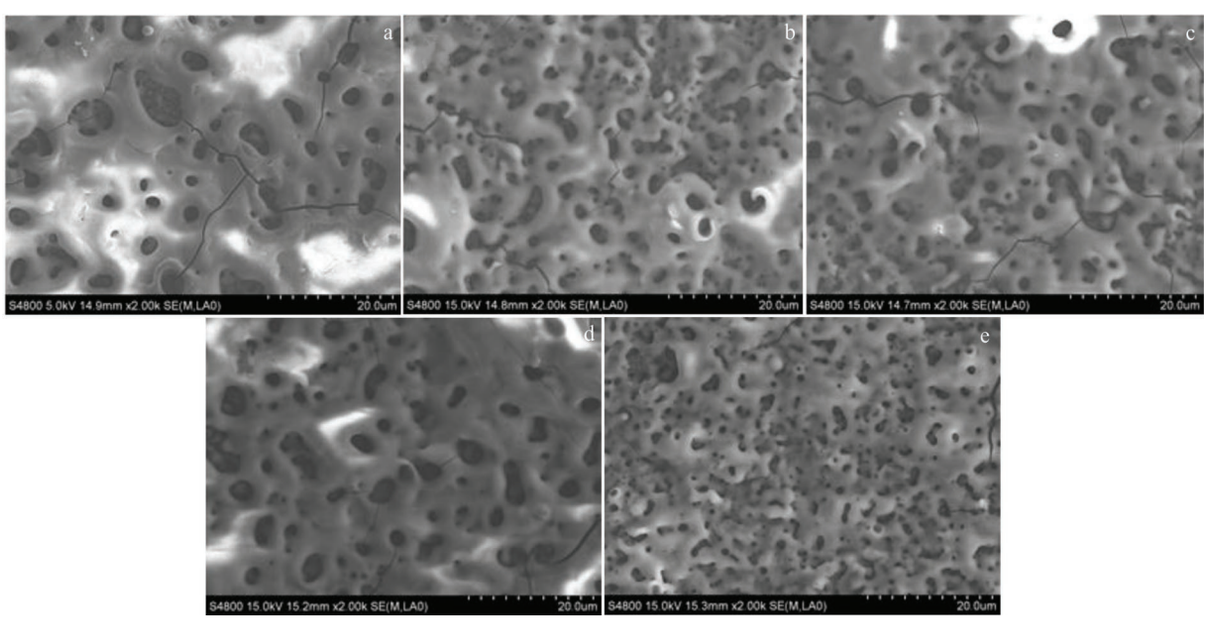

Fig.2 SEM surface morphologies of MAO films after oxidation at 450 °C for 2 h (a), 4 h (b), 6 h (c), 8 h (d), and 10 h (e)

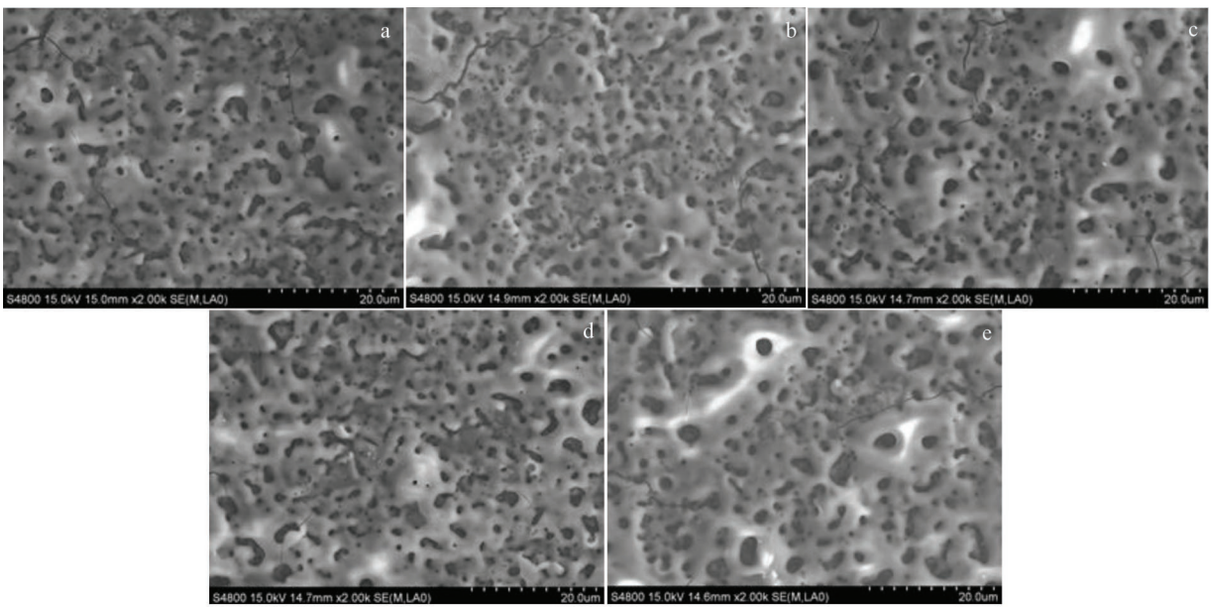

Fig.3 SEM surface morphologies of MAO films after oxidation at 500 °C for 2 h (a), 4 h (b), 6 h (c), 8 h (d), and 10 h (e)

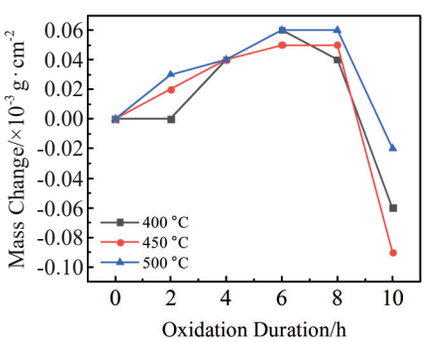

Fig.4 Mass change curves of MAO films after oxidation at different temperatures

g/cm^2. The mass gain is increased with prolonging the oxidation duration, and it tends to be stabilized when the oxidation duration is 6 h. After oxidation for 10 h, the mass is decreased due to the shedding of the film layer.

After oxidation at 500 °C for 2 h, the mass gain is 0.000 03 g/cm^2. The mass gain is increased with prolonging the oxidation duration, and it tends to be stabilized when the oxidation duration is 6 h. After oxidation for 10 h, the mass is slightly decreased due to the shedding of the film layer.

The oxidation kinetics of MAO aluminum alloy film layer can be expressed by the parabolic velocity equation[17], as follows:

$$W^2=2Kt \quad (4)$$

where W represents oxidation mass gain, K is oxidation rate constant, and t is the oxidation time.

After revising the Wagner's empirical formula of oxidation, Eq.(5) can be obtained, as follows:

$$W^n=Kt \quad (5)$$

where n is the oxidation index.

Thus, the relationship between oxidation mass gain and oxidation time and the kinetic relationship of high-temperature oxidation of MAO film layer can be obtained. If $1<n<2$, the oxidation reaction depends not only on the reaction between MAO film and oxygen, but also on the reaction velocity between oxygen and Al[18]. If $n>2$, it can be inferred that MAO film layer can efficiently prevent the high-temperature oxidation. Therefore, in order to determine the difficulty degree of oxidation reaction at high temperature and to quantitatively judge the antioxidant performance, Eq. (6) can be obtained, as follows:

$$K=K_0\exp(-Q/RT) \quad (6)$$

where K_0 is a constant, Q is the oxidation activation energy, R is gas constant, and T is the temperature. The higher the oxidation activation energy, the higher the energy for O diffusion across MAO film surface, i. e., the better the antioxidation performance of MAO film[19].

Table 4 shows the high-temperature oxidation index of MAO film at different temperatures. All the oxidation indexes are above 2, indicating that MAO films show excellent antioxidation performance at high-temperature, and can effectively prevent the O diffusion.

2.3 Surface morphology of MAO film after thermal shock

The thermal shock resistance can directly reflect the influence of periodically changing temperature on the binding force between MAO film and matrix. The higher the thermal

Table 4 High-temperature oxidation indexes of MAO films at different temperatures

Temperature/°C	Oxidation index, n	Oxidation activation energy, Q/kJ·mol^{-1}
400	3.2	
450	2.7	620.4
500	2.3	

shock resistance, the higher the stability of MAO film. The thermal shock failure consists of thermal shock fracture and thermal shock damage, which occurs on the MAO surface in instantaneous heating, resulting in the surface crack or crazing after multiple heating-cooling cycles. The thermal shock failure of MAO film is mainly thermal shock damage.

Fig. 5 shows SEM microstructures of MAO films after thermal shock cycles with air-cooling and water-cooling. After 12 thermal shock cycles with water-cooling at 500 °C, the black spots appear on MAO film, which are inferred as the oxidation products inside MAO film, and their sizes are basically the same with increasing the thermal shock cycles. MAO film does not fall off at the spot positions. After 30 thermal shock cycles with water-cooling at 500 °C, the cracks appear on MAO film surface due to the thermal stress caused by the difference in the thermal expansion coefficients of MAO film layer and the aluminum alloy matrix. The water enters the surface pores and reacts with the film and matrix, forming the lamellar oxide. With the thermal shock cycles further proceeding, the lamellar oxide multiplies and the stacking phenomenon occurs, which facilitates the crack expansion. Besides, MAO film is sensitive to the thermal stress, which further promotes the formation and growth of the internal microcracks. After 60 thermal shock cycles with water-cooling at 500 °C, MAO film on the matrix corners begins to fall off. More water enters the inner part of MAO film, which directly destroys the integrity of MAO film, resulting in more cracks and fracture. Due to the difference in the thermal expansion coefficients of MAO film layer and the aluminum alloy matrix, the upper and lower layers are damaged and then MAO film peels off. The rare earth oxide CeO_2 inside the film layer reduces the amount of water entering the film layers by greatly decreasing the pores during the initial reaction stage, thus releasing partial stress produced by thermal shock and impeding the formation of cracks to some extent. However, with increasing the number of thermal shock cycles, the stress release is not timely, resulting in the film cracking and damage. Moreover, when the specimen is immersed in water, lots of bubbles are generated when the water boils, which produces a transient cavitation effect on the MAO film, thereby promoting the shedding of MAO film layer.

MAO films after thermal shock cycles with air-cooling show better performance than the ones with water-cooling do. After 30 thermal shock cycles with air-cooling, small black spots and small cracks appear on MAO film surface, which is caused by the entrance of water and oxygen in the air into the inner layer of MAO film. After 60 thermal shock cycles with air-cooling, the surface cracks are expanded, the number of black spots is increased, and no obvious damage or peeling occurs, indicating that the thermal shock resistance of MAO films after thermal shock cycles with air-cooling is better than that with water-cooling.

2.4 Thermal shock failure models of MAO film

The thermal shock resistance of MAO films is mainly influenced by the difference in thermal expansion coefficients between MAO film and the matrix, phase transformation, oxidation reaction, and thermal corrosion during the high-temperature oxidation. Among them, the difference in thermal expansion coefficients between MAO film and the matrix is the most influential factor, which generates the thermal stress between layers and induces the crack formation. Thus, MAO film peels off along the direction parallel to the aluminum alloy matrix. The film layer and the matrix can react with H_2O and oxygen, continuously producing a series of new substances, such as oxide and hydroxide, with the thermal shock cycles proceeding. When the production accumulates to a certain level, the film cracks and falls off.

Fig. 6 shows the schematic diagram of the thermal shock failure models of MAO film. It can be seen that the initial MAO film is closely connected to the aluminum alloy matrix with high bonding strength and the flat uniform surface. After several thermal shock cycles, because the inner layer is more sensitive to the thermal stress, the internal tensile stress and

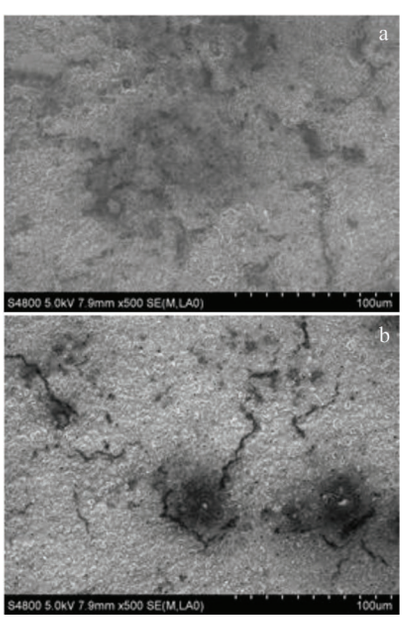

Fig.5 SEM microstructures of MAO films after thermal shock cycles with air-cooling (a) and water-cooling (b)

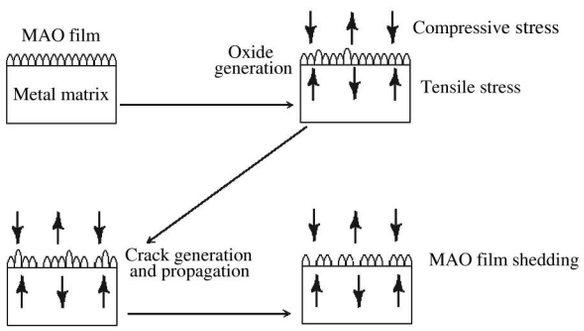

Fig.6 Schematic diagram of thermal shock failure models of MAO films

external compressive stress are exerted jointly onto the interface. Meanwhile, H_2O and O_2 enter the inner film layer, and then the corresponding oxides and hydroxides are formed. With the thermal shock cycles further proceeding, the internal stress concentration occurs and the produced oxides and hydroxides are continuously accumulated due to the continuous internal tensile stress and the influence of external pressure. The cracks appear on MAO film surface and then begin to expand. Finally, when the crack extends across the entire surface, MAO film peels off[20,21].

3 Conclusions

1) The high-temperature oxidation resistance of the micro-arc oxidation film on 2A12 aluminum alloy is decreased with increasing the temperature. The oxidation indexes are all above 2, indicating that the micro-arc oxidation films have excellent antioxidation performance during the high-temperature oxidation and can effectively prevent the oxygen diffusion.

2) The thermal shock resistance of micro-arc oxidation film after thermal shock cycles with air-cooling is better than that with water-cooling. After 60 thermal shock cycles, the micro-arc oxidation film layer suffering water-cooling on the matrix corners begins to fall off, while that suffering air-cooling only has surface cracks without film layer shedding.

3) The thermal shock failure of the micro-arc oxidation film is mainly caused by the difference in thermal expansion coefficients between the film and the matrix and the formation of oxides and hydroxides on the film due to the reaction with H_2O and O_2. CeO_2 in the film layer reduces the pore size, which effectively reduces the influence of thermal shock on the film layer at the initial stage of thermal shock cycles. However, with the thermal shock cycles further proceeding, the subcarbonate and hydroxide are generated, leading to the film failure.

References

1 Wang P, Hu J, Li R Y *et al*. *Rare Metal Materials and Engineering*[J], 2021, 50(1): 56

2 Li H, Song Z H, Tang P. *Rare Metal Materials and Engineering* [J], 2020, 49(3): 755

3 Shao Z C, Zhang Q F, Yang L *et al*. *Materials and Manufacturing Processes*[J], 2015, 30(12): 1505

4 Chen G Q, Liu J P, Shu X *et al*. *International Journal of Heat and Mass Transfer*[J], 2019, 138: 879

5 Shao Zhongcai, Xia Jili, Zhang Yuexiu. *Materials and Manufacturing Processes*[J], 2016, 31(1): 53

6 Shang W, Wang Y Y, Wen Y Q *et al*. *International Journal of Electrochemical Science*[J], 2017, 12(12): 11 875

7 Ma J. *2016 International Conference on Mechatronics, Manufacturing and Materials Engineering*[C]. Les Ulis: EDP Sciences, 2016, 63: 1013

8 Chen Z M, Lu P, Xu J Z *et al*. *Applied Mechanics and Materials* [J], 2012, 190-191: 599

9 Kim J H, Song M J, Lee C J *et al*. *Carbon*[J], 2013, 52: 398

10 Li S H, Liu X, Liu S J. *Journal of Physics: Conference Series*[J], 2020, 1570(1): 12 044

11 Pan M Q, Sheng J, Liu J Z *et al*. *Sensors*[J], 2020, 20(6): 1736

12 Guneri E, Ulutas C, Kirmizigul F *et al*. *Applied Surface Science* [J], 2010, 257(4): 1189

13 Chen X M, Fan Y Y. *IOP Conference Series: Materials Science and Engineering*[J], 2020, 768(2): 22 009

14 Hussein R O, Northwood D O. *Developments in Corrosion Protection*[M]. New York: Intech Open, 2014: 201

15 Yang W, Gao Y, Guo P *et al*. *Journal of the Mechanical Behavior of Biomedical Materials*[J], 2020, 101: 103 448

16 Li Hong, Zhang Jin, Peng Li *et al*. *Surface Technology*[J], 2015, 44(10): 52 (in Chinese)

17 Fang Z G, Cao J Y, Guan Y. *Corrosion Control Technologies for Aluminum Alloy Vessel*[M]. Singapore: Springer, 2020

18 Wang W Z, Feng S S, Li Z M *et al*. *Journal of Materials Research and Technology*[J], 2020, 9(3): 6014

19 Wen Z, Feng T, Ouyang G *et al*. *International Journal of Precision Engineering & Manufacturing*[J], 2018, 19(7): 1081

20 Low I M, Lawrence D, Smith R I. *Journal of the American Ceramic Society*[J], 2005, 88(10): 2957

21 Yu S, Yu Z T. *Biomedical Materials*[J], 2008, 3(4): 44 112

2A12铝合金微弧氧化膜的高温氧化性能

马国峰，李　会，刘志扬，孙世能，王梓垚

(沈阳大学，辽宁 沈阳 110044)

摘　要：对2A12铝合金表面的微弧氧化膜进行了高温氧化实验研究。结果表明：微弧氧化膜层的高温抗氧化性能随着温度的升高而降低，但氧化指数均在2以上，说明微弧氧化膜层对于2A12铝合金起到了保护作用，有效地阻止了高温氧化时的氧扩散。微弧氧化膜层抗空冷热震性能要优于抗水冷热震性能，在60次热震循环后，水冷热震的合金边角处出现膜层脱落现象，而空冷热震的合金只在表面出现裂纹，没有膜层脱落现象出现。微弧氧化膜热震失效主要由膜层与基体热膨胀系数不同、膜层与H_2O、氧气反应分别生成氢氧化物与氧化物所导致；膜层内部的CeO_2起到减小孔径的作用，在热震反应初期能够有效地降低热震对膜层的影响，但随着循环次数增多，生成碱式碳酸盐和氢氧化物，导致微弧氧化膜失效。

关键词：高温抗氧化性能；微弧氧化膜；抗热震性能；稀土氧化物添加剂

作者简介：马国峰，男，1978年生，博士，教授，沈阳大学，辽宁 沈阳 110044，电话：024-62269852，E-mail：guofma@163.com